

# Supplementary Materials for: “Unveiling midcrustal seismic activity at the front of the bolivian altiplano, Cochabamba region.”

G.A. Fernandez<sup>1,\*</sup>, B. Derode<sup>2</sup>, L. Bollinger<sup>3</sup>, B. Delouis<sup>4</sup>, M. Nieto<sup>1</sup>, F. Condori<sup>1</sup>, N. Sarret<sup>1</sup>, J. Letort<sup>5</sup>, S. Godey<sup>3</sup>, M. Wimez<sup>1</sup>, T. Griffiths<sup>1</sup>, W. Arce<sup>1</sup>.

<sup>1</sup> Observatorio San Calixto, La Paz, Bolivia

<sup>2</sup> EOST, ITES UMR 7063, Université de Strasbourg, Strasbourg, France

<sup>3</sup> CEA, DIF, F-91297, Arpajon, France

<sup>4</sup> Géoazur, UMR 7329, Université Cote d’Azur, France

<sup>5</sup> Research Institute in Astrophysics and Planetology | IRAP · DIP

\* Corresponding author: [tonino.gafm@gmail.com](mailto:tonino.gafm@gmail.com)

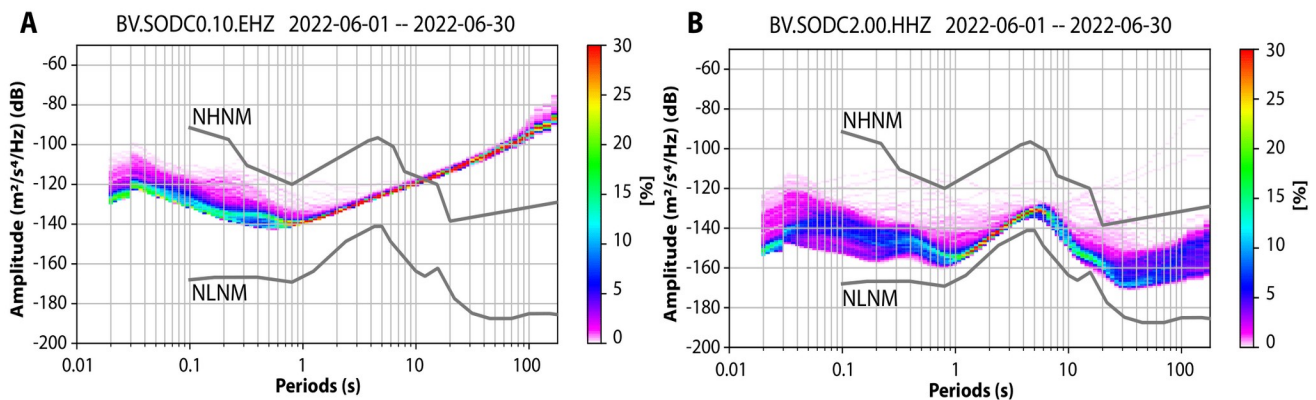
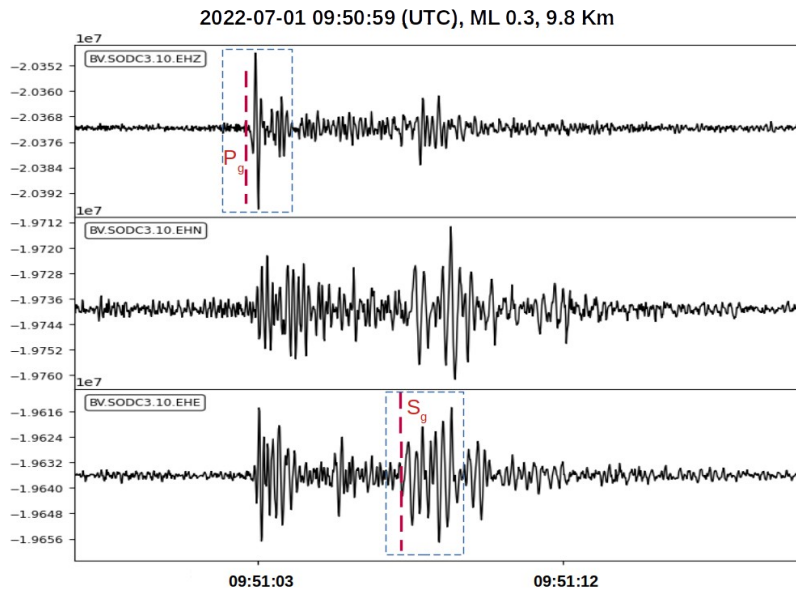


**Figure S1. a.** The L22 short period vertical channel results (SODC0) **b.** The TC-120 broadband vertical results (SODC2), the signals on that period fall between the high and low noise model of Petersen (1993).

a.



b.

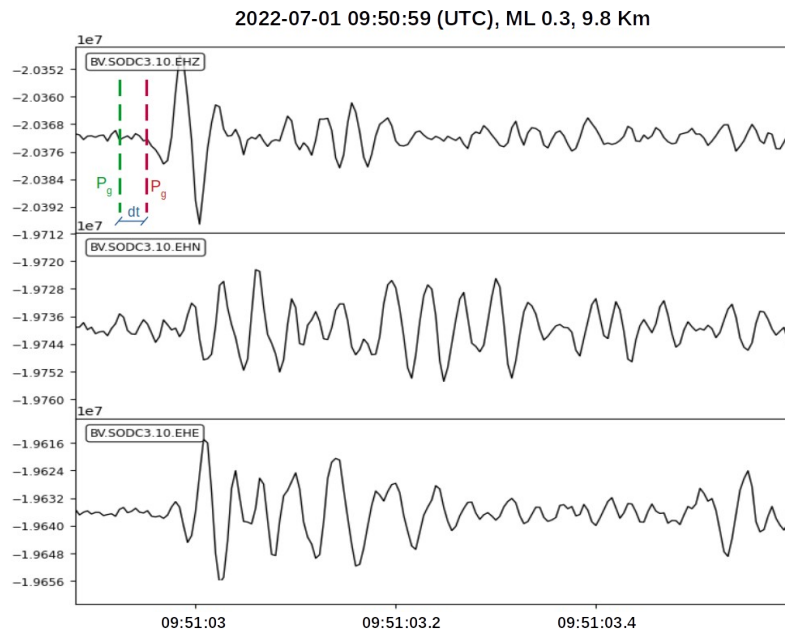


**Figure S2. a.** An example of an automatic pick for  $P_g$  and  $S_g$  (red dashed line), blue dashed line represents the zone of interest to zoom for the quality control. **b.** The  $P_g$  phase zoom to present the manual (green dashed line) versus the automatic pick (red dashed line),  $dt$  represent the delta time difference between two peaks (less than 0.2 seconds)

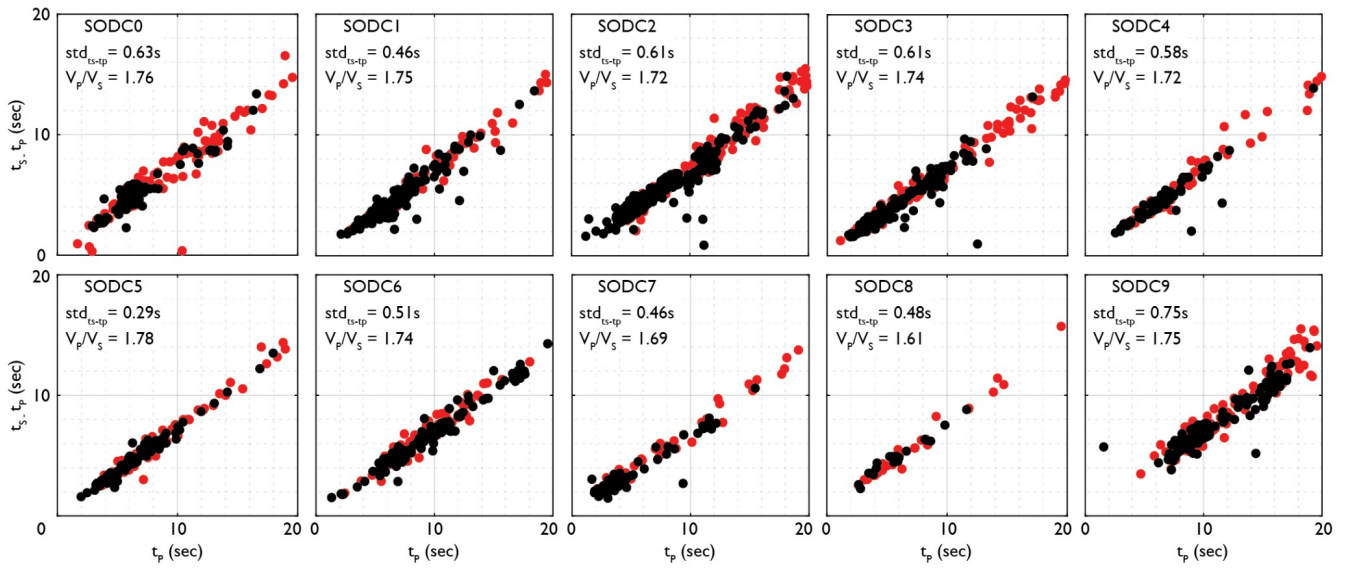
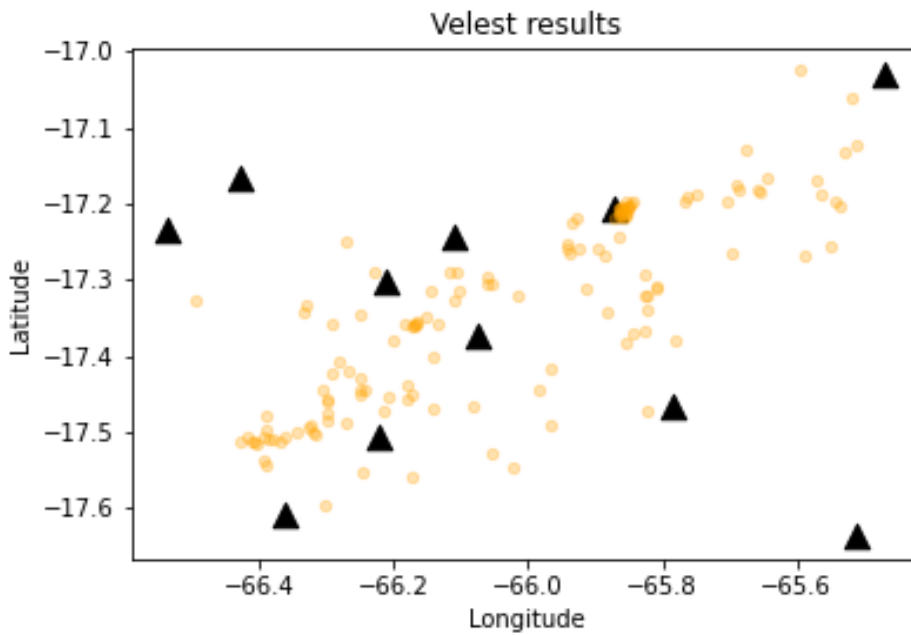
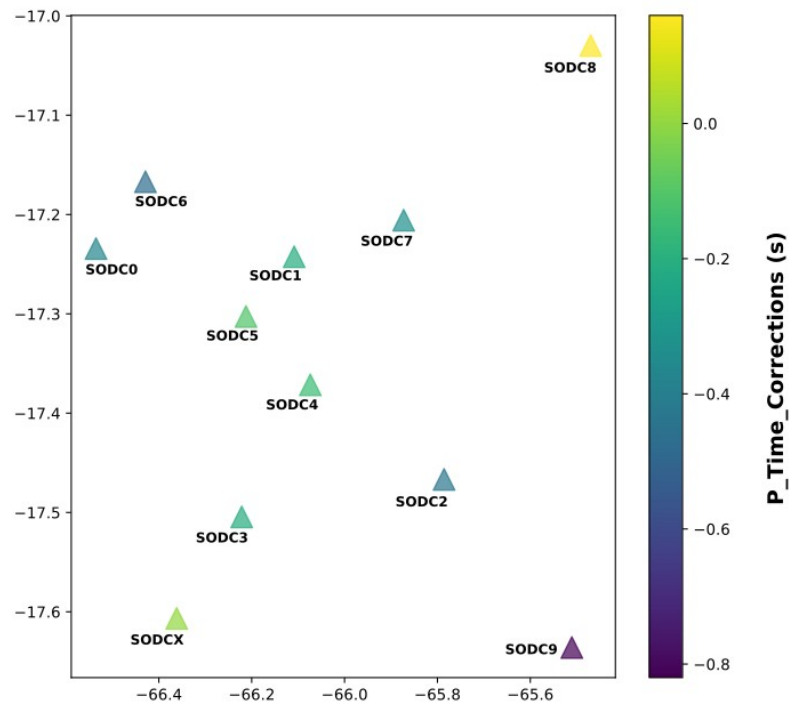


**Figure S3.** Wadati plot for each seismic station. Red dots correspond to manual picks, and black dots to automatic PhaseNet picks. Most of the stations display low standard deviation. SODC0, SODC2, SODC3 and SODC9 display a general deviation  $> 1s$  ( $2\sigma$ ), indicating higher difficulties in wave picking, mainly due to lower signal-to-noise ratio at these stations.

a.



b.



c.

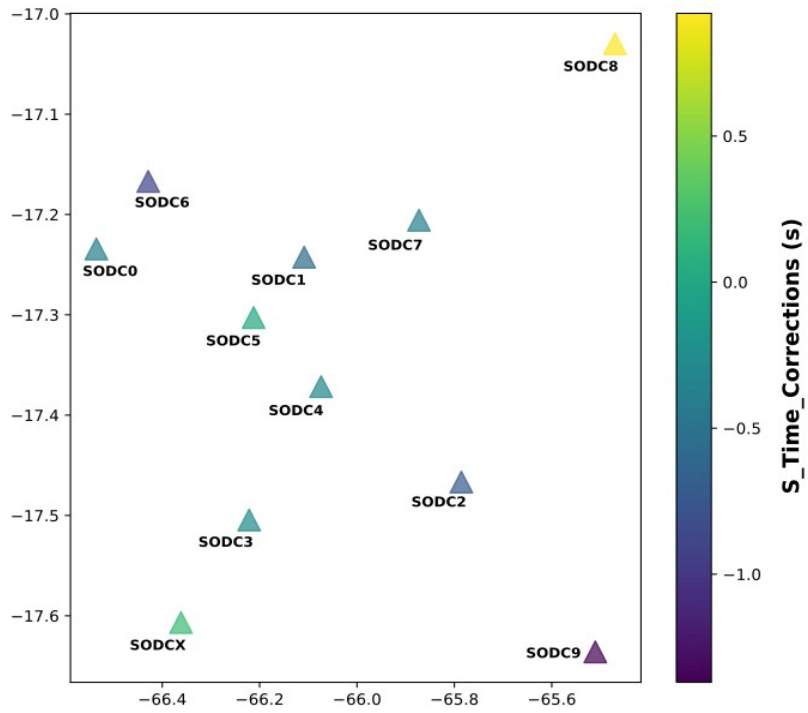


**Figure S4. a.** Seismic events (orange circles) relocated after VELEST algorithm, seismic stations in black triangles, all earthquakes are within the 190°. **b.** The P time correction in seconds for each seismic station. **c.** The S time correction in seconds for each seismic station.

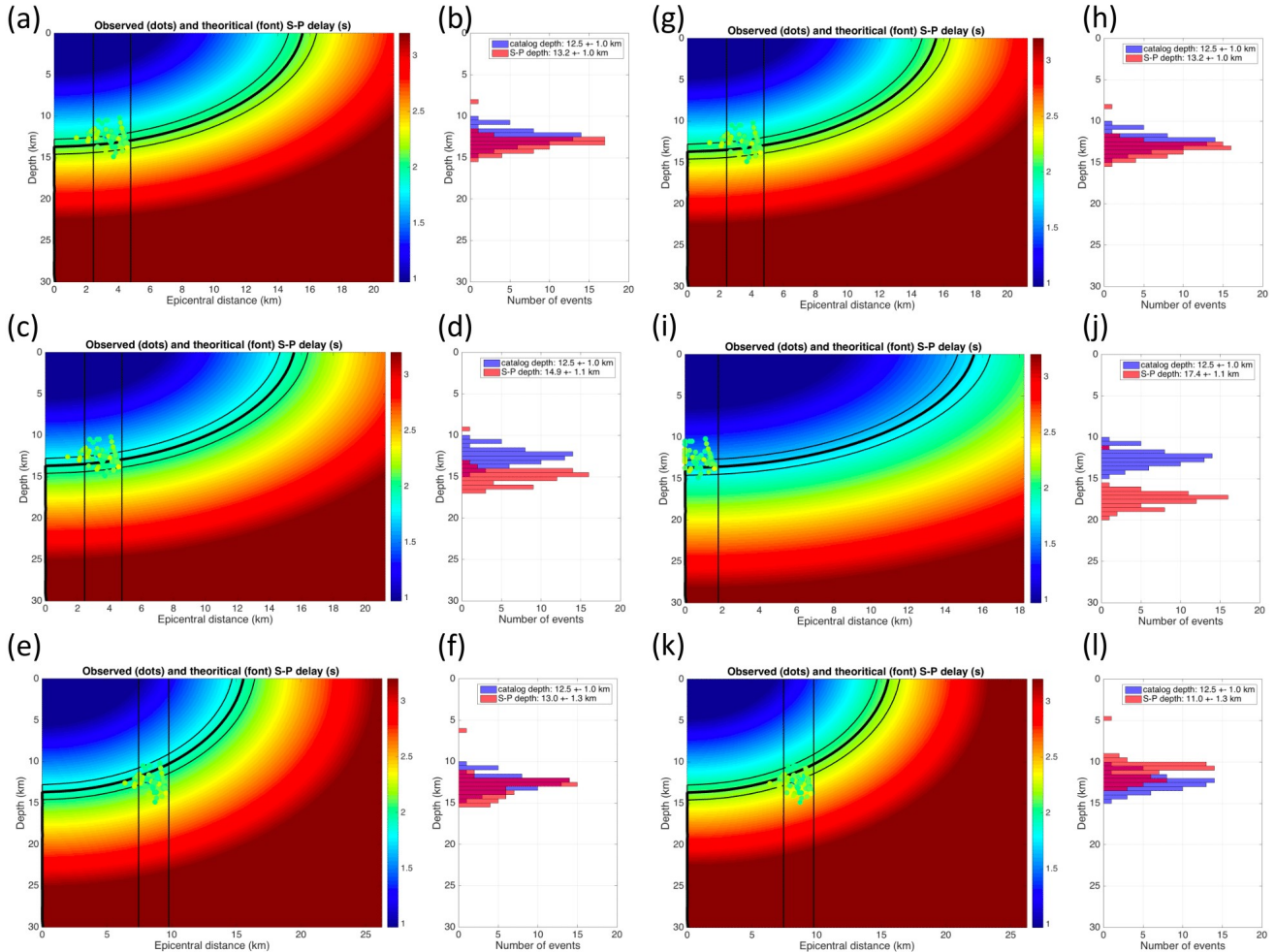


**Figure S5.** S-P delay time for “Cochabamba Norte” cluster (sensitivity test analysis) **a – b.** Results obtained with  $V_p/V_s=1.75$  and 0 km error and its depth histogram comparison. **c – d.** Results obtained with  $V_p/V_s=1.69$  and 0 km error and its depth histogram comparison. **e – f.** Results obtained with  $V_p/V_s=1.75$  and 5 km error. **g – h.** Results obtained with -10% of velocity model variation and its depth histogram comparison. **i – j.** Results obtained with +10% of velocity model variation with a  $V_p/V_s$  of 1.69 and its depth histogram comparison. **k – l.** Results obtained with -10% of velocity model variation with a  $V_p/V_s$  of 1.69 and its depth histogram comparison.

### ***What is the impact of epicenter and velocity model errors on depth estimation? (Figure S5)***

Epicenters are constrained at 5 km (refer to section 3.2.4), and P & S velocities are assumed trustworthy at  $\pm 10\%$ , from VELEST (Table S3d). If, due to localization errors, the epicentral distance is underestimated by 5 km (Figure S5 e - f), the S-P delays will better explain a slightly shallower cluster (13 km). If the P & S velocities are underestimated by 10% but the localization correct (Figure S5 g - h), once again, the S-P delays will better explain a slightly shallower cluster (13.2 km). On the

opposite, with an overestimation of the epicentral distance or an overestimation of the velocities, the S-P delays will explain deeper events. From the provided range of location uncertainty (5km) and velocity model uncertainty (+-10%), with a VP/VS ratio at 1.69, the cluster can be found at a maximum around 17.5 km assuming an overestimated epicentral distance and an overestimated velocity model ( Figure S5 i - j), and at a minimum around 11 km, assuming an underestimated epicentral distance and an underestimated velocity model ( Figure S5 k - l).

This complete analysis of the possible bias from velocity model and location uncertainties on the depth estimation show that, even taking account location & velocities errors that add up for the worse, without offsetting each other, the range of possible average clusters remain constrained between 11 and 17.5 km. The cluster is very likely to be located around 13-15 km, well coherent with the depth found by the FMNEAR waveform inversion (Figure 7).

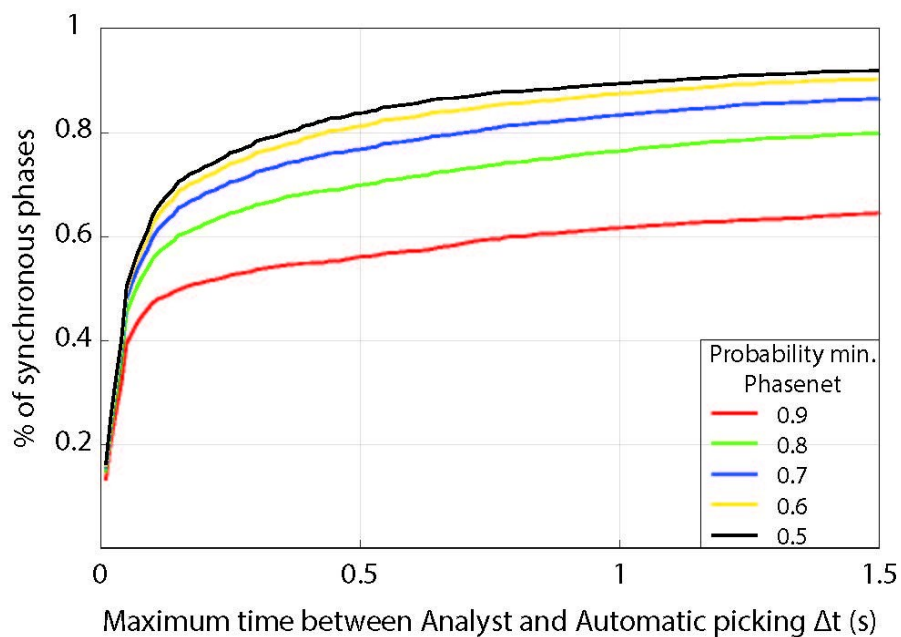


**Figure S6.** Percentage of synchronous phases (Analysts vs Automatic) as a function of Phasenet probability threshold and of the authorized time chosen. At the scale of the whole picks, with a threshold of 0.5, more than 80% of the analysts picks are seen automatically.

### ***FMNEAR Joint Moment Tensor Inversion quality control (Figure S7, S8, S9).***

The Figures S7 and S8 show how the focal mechanism at of the small Cochabamba Centro earthquake is unconstrained by polarities alone, and Figure S9 shows how it is correctly constrained by the joint inversion of polarities and waveforms.

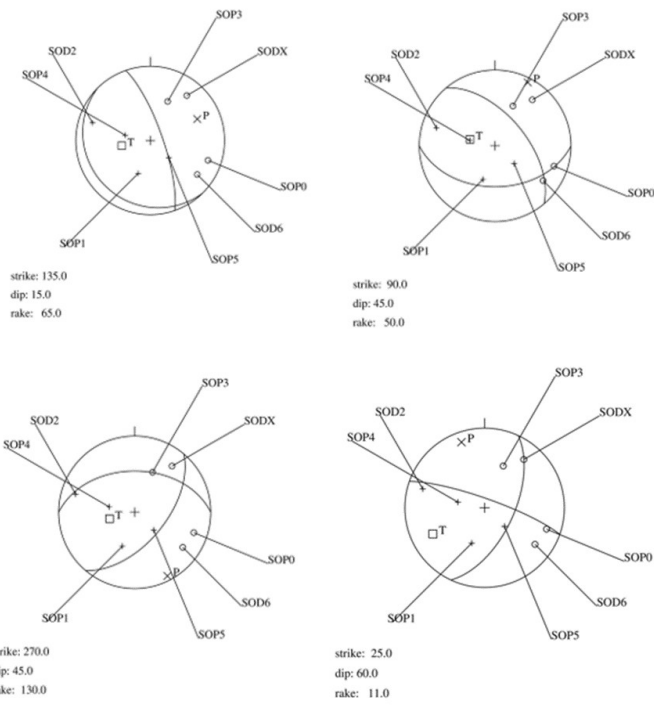
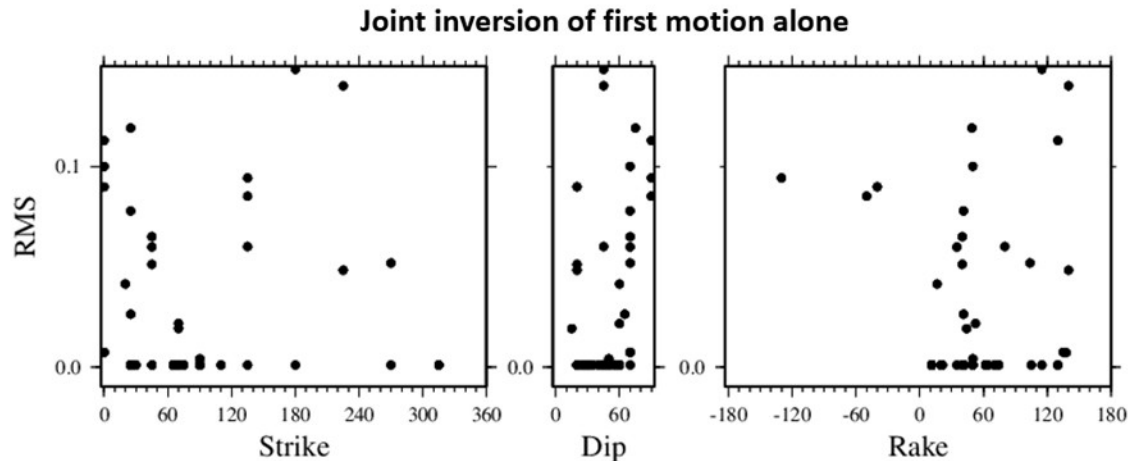


**Figure S7.** Four different focal mechanisms solutions explaining equally well the first motion data, for the 2022/08/14 08:05:06 UTC Mw 2.5 event.

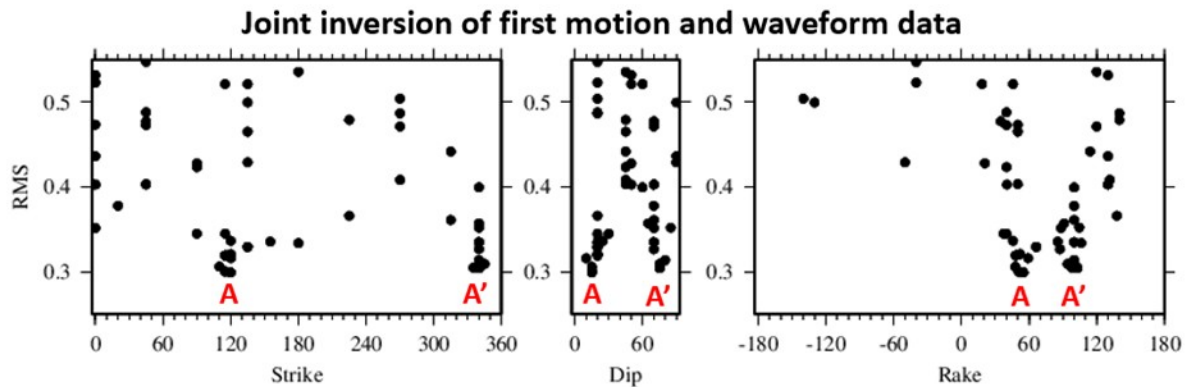
In Figure S8, the best strike, dip and rake solutions from the inversion of polarities alone are plotted as a function of their RMS misfit value. As can be seen, a wide range of strike, dip and rake values is possible, explaining all polarities (RMS = 0), except for negative rakes corresponding to normal faulting solutions.



**Many possibilities in strike, dip, and rake with RMS ~0 (~all polarities explained), with the exception of negative rakes, meaning normal faulting is discarded**

**Figure S8.** Best solutions found at the end of the various grid search and the simulated annealing combinations for the inversion of first motion data alone, for the 2022/08/14 08:05:06 UTC Mw 2.5 event.

When we invert the first motion and waveform data jointly, the solution becomes much better constrained, as shown by Figure S9, which is similar to Figure S8 except that it is obtained by the joint inversion. The RMS values are higher because the waveforms are never perfectly matched due in particular to the inadequacy of the velocity model and the presence of residual noise in the data despite the filtering. This time we obtain two groups of solutions, named A and A', which in fact correspond to the same mechanism. The solution is therefore well constrained.



**A and A' are the two nodal planes of the same focal mechanism  
→ the solution is quite unique**

**Figure S9.** Best solutions found at the end of the various grid search and the simulated annealing combinations for the joint inversion of first motion and waveform data, for the 2022/08/14 08:05:06 UTC Mw 2.5 event. Only the waveforms of the four nearest stations are used.

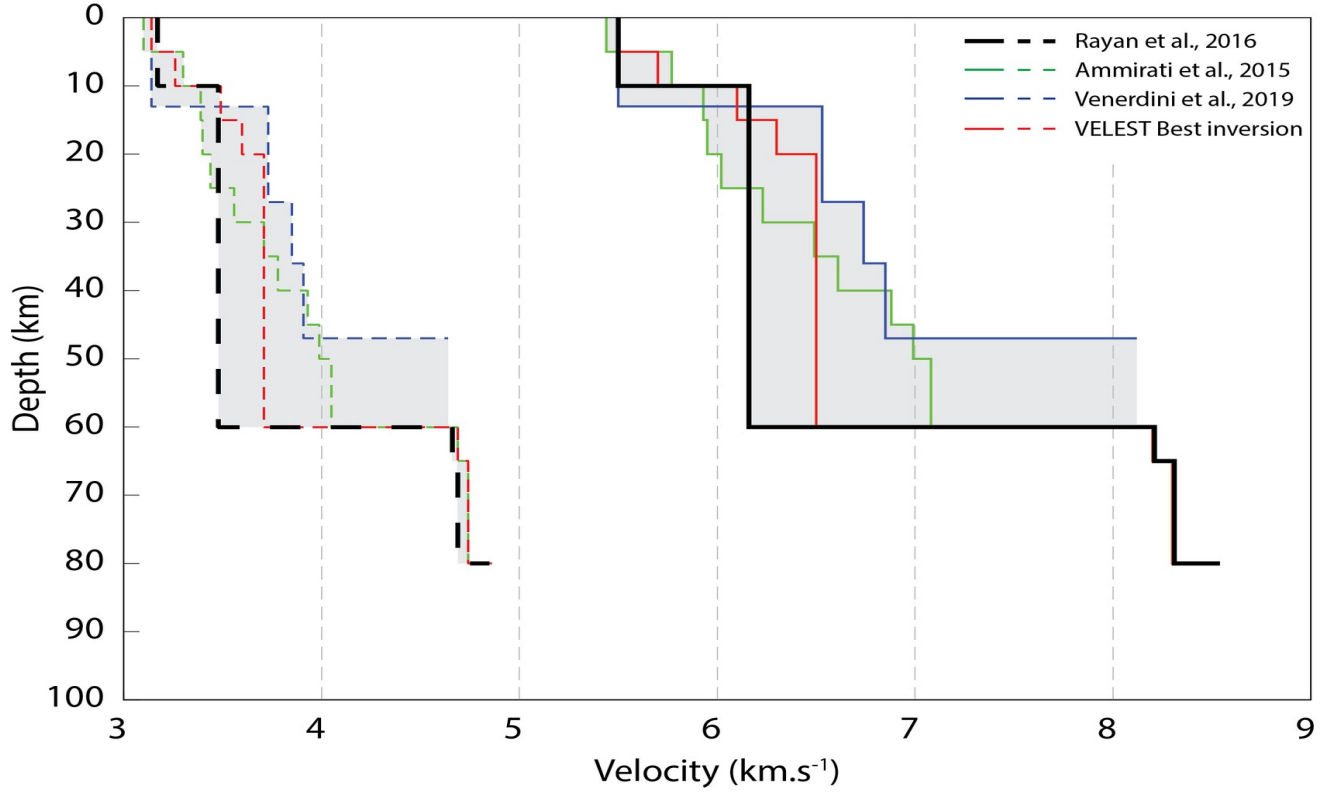


**Figure S10.** The velocity models tested in this project: Ryan et al. 2016 (black), Ammirati et al. 2015 (green), Venerdini et al. 2019 (blue) and the improved velocity taken from VELEST computation (red).

**Table S1.** Seismic station geographical locations and its main characteristics.

Station Code	Latitude (°)	Longitude (°)	Elevation (m)	Site	Type	Start Date	SPS / Digital Rate	Data Availability
SODC0	-17.234	-66.535	3076	Cochabamba/Morochata	SP-L22	24/04/2022	100 /32 Bits	100.00%
SODC1	-17.243	-66.108	3940	Cochabamba/Kehuina Chico	SP-L22	25/04/2022	100 /32 Bits	100.00%
SODC2	-17.467	-65.786	2980	Cochabamba/Curzani	BB-TC120	23/04/2022	100 /32 Bits	100.00%
SODC3	-17.505	-66.222	3103	Cochabamba/Cuturita	SP-L22	31/03/2022	100 /32 Bits	100.00%
SODC4	-17.372	-66.074	2829	Cochabamba/Sacaba	SP-L22	05/04/2022	100 /32 Bits	100.00%
SODC5	-17.303	-66.212	3311	Cochabamba/Cruzani	SP-L22	21/04/2022	100 /32 Bits	100.00%
SODC6	-17.167	-66.429	4264	Cochabamba/Peñas	BB-TC120	22/04/2022	100 /32 Bits	100.00%
SODC7	-17.206	-65.873	2609	Cochabamba/Pampa Tambo	BB-TC120	06/04/2022	100 /32 Bits	100.00%
SODC8	-17.030	-65.471	376	Cochabamba/Padresama	SP-L22	26/04/2022	100 /32 Bits	80.00%
SODC9	-17.636	-65.511	3340	Cochabamba/Torowarku	BB-TC120	27/04/2022	100 /32 Bits	100.00%
SODCX	-17.607	-66.362	2867	Cochabamba/Parotani	BB-6TD	11/08/2022	100 /32 Bits	100.00%

**Table S2.** The P / S precision (P), recall (R), F1 values calculated after phases association on the 2 catalogues considered (analysts and automatic). The NTP (number of true positives), NFP (number of false positives), and NFN (number of false negatives) are also documented.

	<b>P</b>	<b>S</b>
<b>Precision</b>	0.987	0.988
<b>Recall</b>	0.995	0.991
<b>F1</b>	0.991	0.990
<b>NTP</b>	2550	1700
<b>NTN</b>	33	20
<b>NFN</b>	14	15

**Table S3. a.** Velocity model for Cochabamba region deduced from Ryan et al. (2016). **b.** Velocity model for North Argentina proposed by Ammirati et al. (2015). **c.** Velocity model proposed for northwestern Argentina by Venerdini et la. (2020). **d.** Velocity model for Cochabamba region computed by VELEST on this dataset.

**a.**

<b>Vp (km/s)</b>	<b>Vs (km/s)</b>	<b>Depth (km)</b>
5.50	3.17	0
6.16	3.48	10
8.21	4.66	60
8.31	4.69	65
8.54	4.85	80

**b.**

<b>Vp (km/s)</b>	<b>Vs (km/s)</b>	<b>Depth (km)</b>
5.44	3.1	0
5.77	3.3	5
5.93	3.39	10
5.95	3.4	15
6.02	3.44	20
6.23	3.56	25
6.49	3.71	30
6.61	3.78	35
6.88	3.93	40
6.99	3.99	45
7.08	4.05	50
8.20	4.69	60
8.30	4.74	65
8.50	4.86	80

**c.**

<b>Vp (km/s)</b>	<b>Vs (km/s)</b>	<b>Depth (km)</b>
5.50	3.14	0
6.53	3.73	13
6.74	3.85	27
6.85	3.91	36
8.12	4.64	47

**d.**

<b>Vp (km/s)</b>	<b>Vs (km/s)</b>	<b>Depth (km)</b>
5.50	3.14	0
5.70	3.26	5
6.10	3.49	10
6.30	3.6	15
6.5	3.71	20
8.20	4.69	60
8.30	4.74	65
8.50	4.86	80